Review

Cardiac Imaging Techniques for Physicians: Late Enhancement

CME

Peter Kellman, PhD* and Andrew E. Arai, MD

This article is accredited as a journal-based CME activity. If you wish to receive credit for this activity, please refer to the website: www.wileyblackwellcme.com

ACCREDITATION AND DESIGNATION STATEMENT

Blackwell Futura Media Services designates this journal-based CME activity for a maximum of 1 *AMA PRA Category 1 Credit*[TM]. Physicians should only claim credit commensurate with the extent of their participation in the activity.

Blackwell Futura Media Services is accredited by the Accreditation Council for Continuing Medical Education to provide continuing medical education for physicians.

EDUCATIONAL OBJECTIVES

Upon completion of this educational activity, participants will be better able to describe the current state of the art and clinical protocols for late enhancement cardiac imaging techniques.

ACTIVITY DISCLOSURES

No commercial support has been accepted related to the development or publication of this activity.

Faculty Disclosures:

The following contributors have no conflicts of interest to disclose:

Editor-in-Chief: C. Leon Partain, MD, PhD

CME Editor: Scott B. Reeder, MD, PhD

CME Committee: Scott Nagle, MD, PhD, Pratik Mukherjee, MD, PhD, Shreyas Vasanawala, MD, PhD, Bonnie Joe, MD, PhD, Tim Leiner, MD, PhD, Sabine Weckbach, MD, Frank Korosec, PhD

Authors: Peter Kellman, PhD, Andrew E. Arai, MD

This manuscript underwent peer review in line with the standards of editorial integrity and publication ethics maintained by *Journal of Magnetic Resonance Imaging*. The peer reviewers have no relevant financial relationships. The peer review process for *Journal of Magnetic Resonance Imaging* is double-blinded. As such, the identities of the reviewers are not disclosed in line with the standard accepted practices of medical journal peer review.

Conflicts of interest have been identified and resolved in accordance with Blackwell Futura Media Services's Policy on Activity Disclosure and Conflict of Interest. No relevant financial relationships exist for any individual in control of the content and therefore there were no conflicts to resolve.

INSTRUCTIONS ON RECEIVING CREDIT

For information on applicability and acceptance of CME credit for this activity, please consult your professional licensing board.

This activity is designed to be completed within an hour; physicians should claim only those credits that reflect the time actually spent in the activity. To successfully earn credit, participants must complete the activity during the valid credit period.

Follow these steps to earn credit:

- Log on to www.wileyblackwellcme.com
- Read the target audience, educational objectives, and activity disclosures.
- Read the article in print or online format.
- Reflect on the article.
- Access the CME Exam, and choose the best answer to each question.
- Complete the required evaluation component of the activity.

This activity will be available for CME credit for twelve months following its publication date. At that time, it will be reviewed and potentially updated and extended for an additional period.

Late enhancement imaging is used to diagnose and characterize a wide range of ischemic and nonischemic cardiomyopathies, and its use has become ubiquitous in the cardiac MR exam. As the use of late enhancement imaging has matured and the span of applications has widened, the demands on image quality have grown. The characterization of subendocardial MI now includes the accurate quantification of scar size, shape, and characterization of borders which have been shown to have prognostic significance. More diverse patterns of late enhancement including patchy, mid-wall, subepicardial, or diffuse enhancement are of interest in diagnosing nonischemic cardiomyopathies. As clinicians are examining late enhancement images for more subtle indication of fibrosis, the demand for lower artifacts has increased. A range of new techniques have emerged to improve the speed and quality of late enhancement imaging including: methods for acquisition during free breathing, and fat water separated imaging for characterizing fibrofatty infiltration and reduction of artifacts related to the presence of fat. Methods for quantification of T1 and extracellular volume fraction are emerging to tackle the issue of discriminating globally diffuse fibrosis from normal healthy tissue which is challenging using conventional late enhancement methods. The aim of this review will be to describe the current state of the art and to provide a guide to various clinical protocols that are commonly used.

Key Words: late enhancement; delayed enhancement; gadolinium; cardiac magnetic resonance imaging; myocardial infarction; viability

LATE GADOLINIUM ENHANCEMENT, often referred to as simply late enhancement imaging or delayed enhancement, has become a gold standard in myocardial viability assessment (1,2). Late enhancement imaging provides excellent depiction of myocardial infarction (MI) and macroscopic scarring. The use of late enhancement in the diagnosis of ischemic heart disease and in guiding therapy such as revascularization has gained wide acceptance. More recently, late enhancement is playing a broader role in characterizing fibrosis in nonischemic cardiomyopathies (3,4), and in measurement of scar resulting from treatment such as electrophysiology guided ablation (5).

Late enhancement imaging is used to diagnose and characterize a wide range of ischemic and nonischemic cardiomyopathies, and its use has become ubiquitous in the cardiac MR exam. As the use of late enhancement imaging has matured and the span of applications has widened, the demands on image quality have grown. To gain a better understanding of the imaging requirements and technical challenges, it is worthwhile to examine the range of applications and variety of late enhancement patterns (Fig. 1). As imaging techniques have improved, the characterization of subendocardial MI now includes the accurate quantification of scar size, shape, and characterization of borders which have been shown to have prognostic significance (6–10). More diverse patterns of late enhancement including patchy, mid-wall, subepicardial, or diffuse enhancement are of interest in diagnosing nonischemic cardiomyopathies such as ARVD, HCM, DCM, myocar-

ditis, sarcoidosis, amyloidosis, and muscular dystrophy (3,11–17). As clinicians are examining late enhancement images for more subtle indication of fibrosis, the demand for lower artifacts has increased.

A range of new techniques have emerged to improve the speed and quality of late enhancement imaging. These include single shot imaging and motion corrected averaging for acquisition during free breathing, and fat water separated imaging for characterizing fibrofatty infiltration and reduction of artifacts related to the presence of fat. Using conventional late enhancement methods it is difficult to discriminate globally diffuse fibrosis from normal healthy tissue. Methods for quantification of T1 and extracellular volume fraction are emerging to tackle this issue. In light of the numerous new developments and growth of applications, the aim of this review will be to describe the current state of the art and to provide a guide to various clinical protocols that are commonly used. Current limitations and challenges will be described as well as approaches that are emerging.

PHYSIOLOGIC BASIS FOR LATE CONTRAST ENHANCEMENT

Contrast enhancement using gadolinium (Gd) agents is based on T1-shortening and the distribution of contrast agent within the tissue. The mechanism of early and late enhancement relates to the different wash-in and wash-out kinetics of normal myocardium and tissue with myocardial infarction or fibrosis (18,19). Following administration of a bolus of gadolinium contrast agent, the contrast will reach the various tissue compartments within the myocardium at different rates until a dynamic steady state is reached (Fig. 2). The commonly used Gd based contrast agents with large molecular weight are extracellular and will generally take a longer time to wash-in and-out of the infarcted tissue than normal healthy cells. Gadolinium will take even longer to reach regions that have microvascular obstruction (MVO).

The extracellular volume fraction (ECV) in regions of infarcted myocardium (Fig. 3) is significantly higher than that of regions with normal healthy cells and thus have a higher concentration of gadolinium. In the case of acute MI with rupture of the cell membrane, the gadolinium enters the extracellular space and what had previously been intracellular space. For chronic MI with cell replacement by a matrix of collagen the extracellular space is substantially increased. There is a linear relationship between the relaxation rate of longitudinal magnetization ($R1 = 1/T1$) and the change in contrast agent concentration, $\Delta R1 = R1_{post} - R1_{pre} = \gamma [Gd]$ ($\gamma = 4.5$ L mmol^{-1}s^{-1}). Regions with a greater extracellular volume fraction (ECV) will have a higher concentration of contrast agent ([Gd]) at steady state and will experience greater T1-shortening. These images will appear brighter on T1-weighted images, for example using inversion recovery. For example, with a dose of 0.15 mmol/kg, 8% blood by weight, 1.06 kg/L blood density, ECV = 25% for normal tissue, the initial gadolinium concentration would
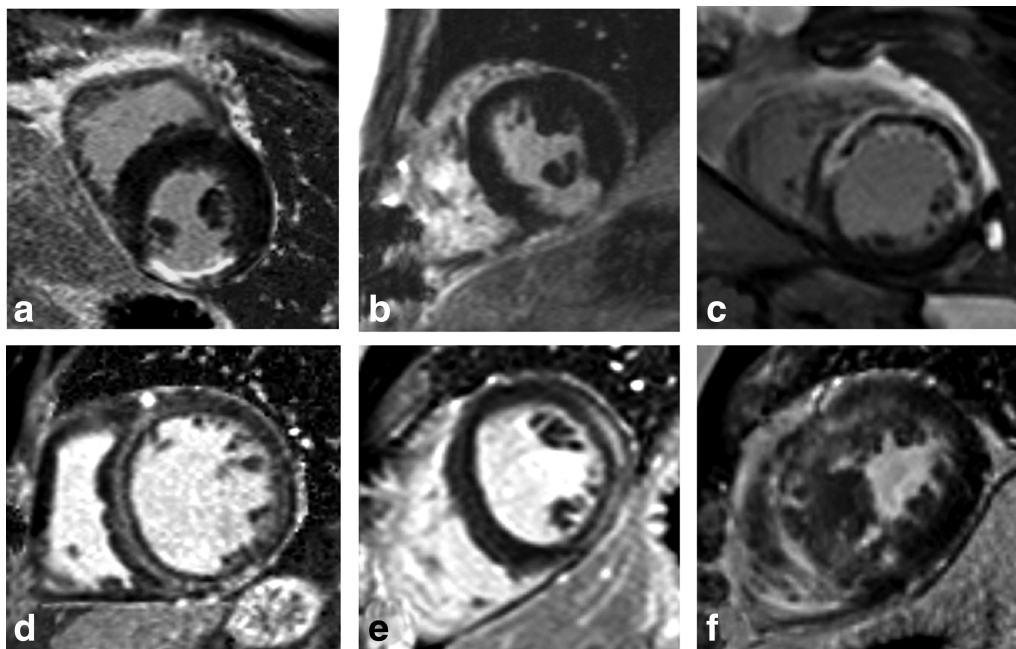
Figure 1. Examples of late enhancement images illustrating a variety of late enhancement patterns: (**a**) subendocardial chronic MI, (**b**) transmural chronic MI, (**c**) acute MI with dark core due to microvascular obstruction, (**d**) mid-wall enhancement in patient with myocarditis, (**e**) subepicardial enhancement in patient with myocarditis, and (**f**) patchy appearance of scarring in a patient with HCM.

be approximately 0.5 mmol/L, and $\Delta R1 = 2.25\ s^{-1}$, which shortens the T1 from nominal 950 ms to approximately 300 ms. At 10 min following contrast administration, the T1 for normal myocardium will decrease to approximately 400 ms depending on the rate of Gd clearance.

Edematous myocardial tissue that may result from acute myocarditis or bordering acute MI (salvage area) will also have increased ECV and correspondingly higher concentration of gadolinium. In the case of

acute MI, the edematous tissue will experience a more rapid early enhancement than the central core. Thus, the early enhancement may show the area at risk (20). The edematous region becomes less conspicuous at a later time (20–30 min) due to the contrast kinetics. In the edematous region, the higher initial concentration of free water and therefore elevated pre-contrast T1 will reduce the net change in relaxivity $\Delta R1$ and thus reduce the effective T1-shortening and apparent contrast enhancement. For this reason, late
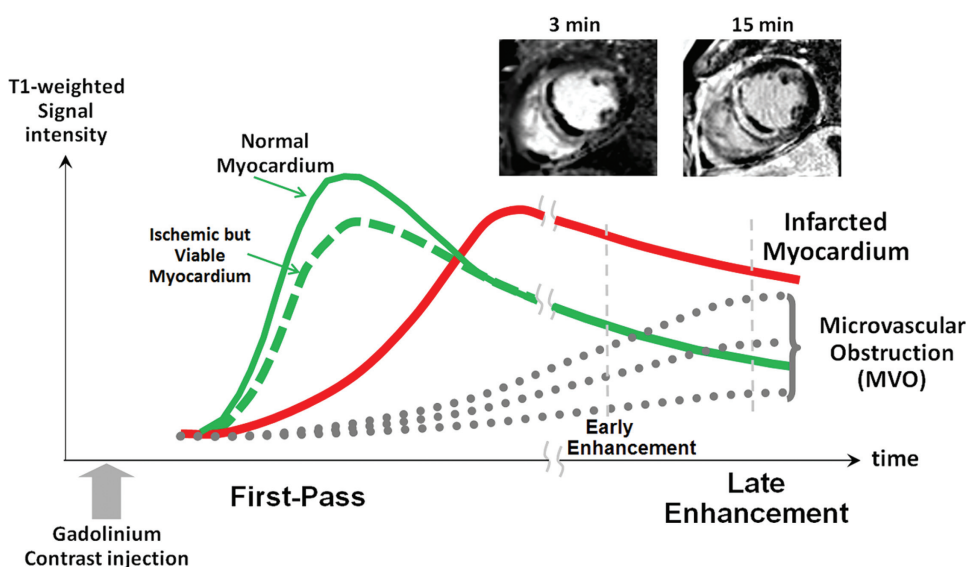

Figure 2. Signal intensity time course from administration of bolus through late enhancement illustrating slower wash-in and wash-out of Gd contrast into infarcted tissue compared with normal ischemic tissue. Tissue with microvascular obstruction (MVO) experiences very slow wash-in of Gd. The apparent size of MVO region in acute MI shrinks between early (3 min) and late (15 min) enhancement images due to late arrival of Gd.
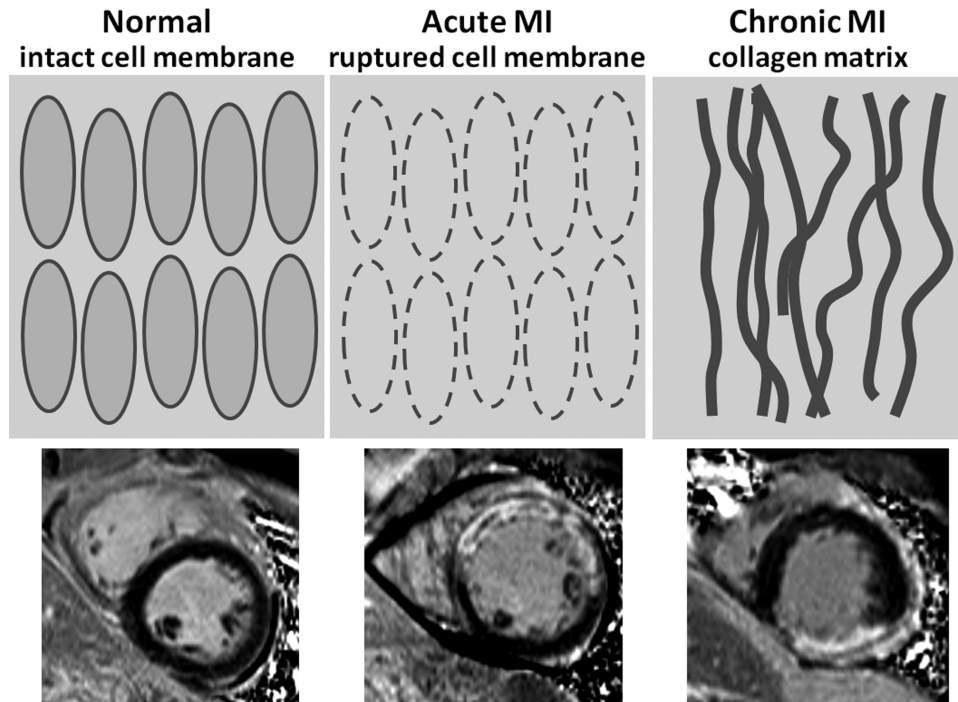
Normal
intact cell membrane

Acute MI
ruptured cell membrane

Chronic MI
collagen matrix

Figure 3. Illustration of extracellular volume fraction for normal myocardium with intact cell membrane, acute MI with ruptured cell membrane, and chronic MI with collagen matrix.

enhancement is less sensitive to the edematous border. Consequently, care must be taken when measuring the size of acute MI to properly account for the kinetics of the border zone (20,21). Although both acute and chronic MI will exhibit late enhancement, they may be distinguished by the presence of edema causing elevated T1 (22) and T2 (23) as measured before contrast administration.

Late enhancement imaging is typically performed 10–30 min following administration of gadolinium when there is sufficient contrast between normal and infarcted tissue. Some data suggest that 20–30 min postcontrast might be more appropriate for acute MI. For detection of subendocardial MI bordering the blood pool, the MI-to-blood contrast is also an important factor and is dependent on several variables including the rate of gadolinium clearance, the percentage of hematocrit, the ECV of the MI, and several imaging protocol parameters. Presence of MVO in acute MI is an important prognostic indicator (24), which is often observed as a dark core (no reflow zone) in the MI due to lower [Gd]. Depending on the severity of MVO, this may not be apparent at 10–20 min. following the bolus, and may be detected with greater sensitivity at an earlier time point. For this reason, it is useful to perform both early and late enhancement imaging as described later.

REQUIREMENTS DISCUSSION

A general discussion of imaging requirements will set the stage for the describing various technical methods. The assessment of viability using late enhancement involves the reliable detection of MI and the measurement of the extent and transmurality (25). This requires full heart coverage and adequate spatial and temporal resolution. Spatial resolution on the order 1.5–2 mm is readily achievable and is generally satisfactory for left ventricular myocardium; however, improved resolution on the order of 1 mm is useful for detecting scar in thin walls such as the RV or atria. Temporal resolution on the order of 150–200 ms is readily achievable in clinically relevant breath-hold protocols (10–15 s), which is generally adequate to avoid motion induced blurring for most subjects. At higher heart rates, protocols must be adjusted for improved temporal resolution.

Adequate contrast between the blood pool and subendocardial MI is important for detection of small MIs and for accurate measurement of MI size. Correction for surface coil intensity variation is also important for methods based on full-width-half maximum (6–8). Increased interest in quantifying the MI border zone region (9,10) and characterizing MI shape have led to demands for improved image quality in terms of SNR and artifacts. Characterization of the edematous border zone in acute MI corresponding to the salvage area, as well as detection of microvascular obstruction, may require measurements at several time points following contrast administration due to the kinetics of contrast wash-in and wash-out. This has implications for the clinical workflow and places demands on rapid imaging to avoid patient fatigue.

The characterization of late enhancement in patients with nonischemic cardiomyopathies places stringent demands on image quality to distinguish true tissue enhancement from artifacts. Diffuse or patchy patterns of enhancement require higher SNR
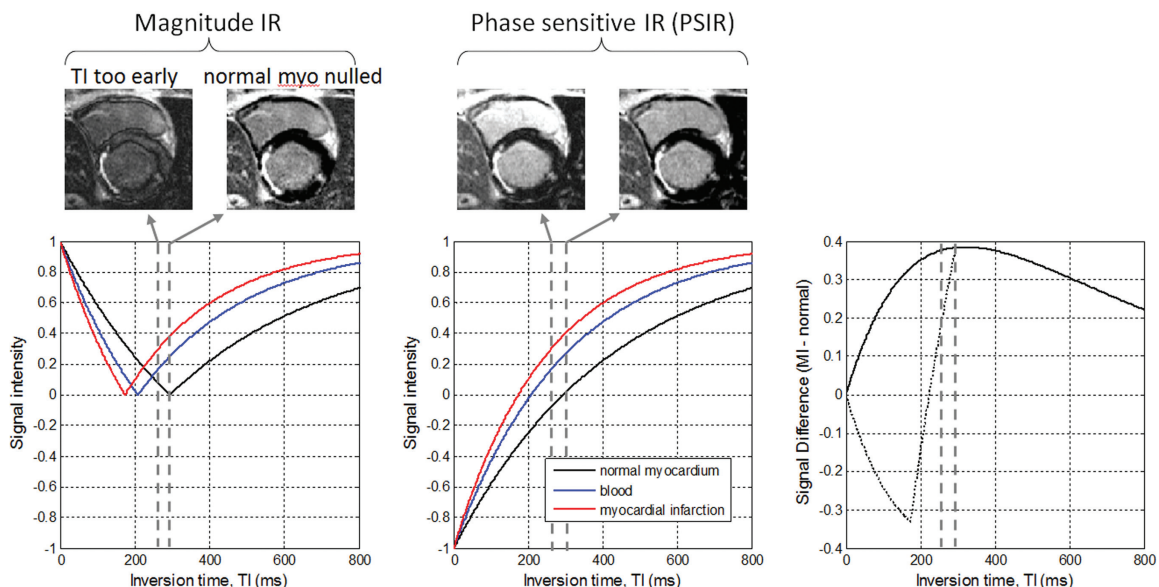
Figure 4. Signal intensity versus inversion time is plotted for magnitude inversion recovery (MagIR) (left) and phase sensitive inversion recovery (PSIR) (center), and signal difference between MI and normal myocardium (right) illustrates the sensitivity of MagIR to setting the inversion time (TI) to null the normal myocardium. MagIR exhibits a loss of contrast and polarity artifact when the TI is too early, whereas PSIR maintains a similar appearance.

to reliably detect. Mid-wall enhancement may be confused with artifacts such as Gibb's ringing or improper setting of TI in magnitude reconstructed images. Subepicardial enhancement may be difficult to distinguish from epicardial fat. The ability to discriminate gadolinium enhancement from intramyocardial fat is important for both ischemic and nonischemic cardiomyopathies due to the process of fatty replacement in scar tissue. These topics are discussed in greater detail in the following presentation of late enhancement imaging, but remain a limitation for many clinical protocols in current use.

The requirement for late enhancement imaging of the atria or other thin walled structures is very demanding, and leads to the need for three-dimensional (3D) imaging (5). In these applications, it would be desirable to have isotropic resolution to perform retrospective multiplanar reformatting and to maintain a high in-plane resolution.

Finally, the ability to cope with patients that are unable to breath-hold or have arrhythmias or significant variation in R-R period is critical in the clinical environment and leads to additional demands on late enhancement imaging.

IMAGING

Choice of Sequence

Inversion recovery (IR) or phase sensitive inversion recovery (PSIR) using ECG gated, segmented FLASH readout, also referred to as spoiled gradient recalled echo (SPGR), have become the most widely used sequences for late enhancement (26,27). Simonetti (28) compared a variety of T1-weighted late enhancement sequences from the standpoint of contrast-to-noise ratio (CNR) and contrast-enhancement ratio

(CER) and determined that IR sequences provided the best CNR and CER, when compared with other T1-weighted methods such as magnetization driven (MD) steady state FLASH or turbo-spin echo (TSE), also known as fast spin echo (FSE). More recently, the use of IR or PSIR with single shot steady state free precession (SSFP), also known as true-FISP or balanced-TFE, has become popular for rapid multislice coverage (29) or in cases for which patients have arrhythmias or difficulty breath-holding (30–35). Navigated free-breathing, segmented 2D late enhancement is an alternative approach to dealing with respiratory motion (36). The basic segmented 2D IR-FLASH and single shot 2D IR-SSFP sequences will be reviewed in more detail, followed by a discussion of protocols. Several sequences variations will be presented.

Inversion recovery images are typically acquired in mid to late diastole to minimize cardiac motion. The inversion recovery time is typically chosen to null the normal myocardium which provides the best tissue contrast between MI and normal myocardium in the case of magnitude image reconstruction (Fig. 4). Normal myocardium will appear black, and the MI with higher gadolinium concentration and consequently shorter T1 and faster recovery will appear bright. The gadolinium concentration in the blood is often at an intermediate concentration dependent on several factors, and thus would have intermediate signal intensity. The signal intensity following inversion recovers exponentially and may be written approximately as $S = abs(1 - 2exp(-TI/T1))$ where the abs() denotes the absolute value for the case of magnitude image reconstruction, TI is the inversion time, and T1 is the longitudinal relaxation parameter. This formula ignores the influence of the readout. The tissue is nulled for $TI = T1 \ln(2) = 0.69 \, T1$, where ln() is the natural logarithm. The TI may be determined by multiple

inversion time set early   normal myocardium nulled   inversion time set late

270 290 310 350 340 370 390 410
Magnitude images

270 290 310 350 340 370 390 410
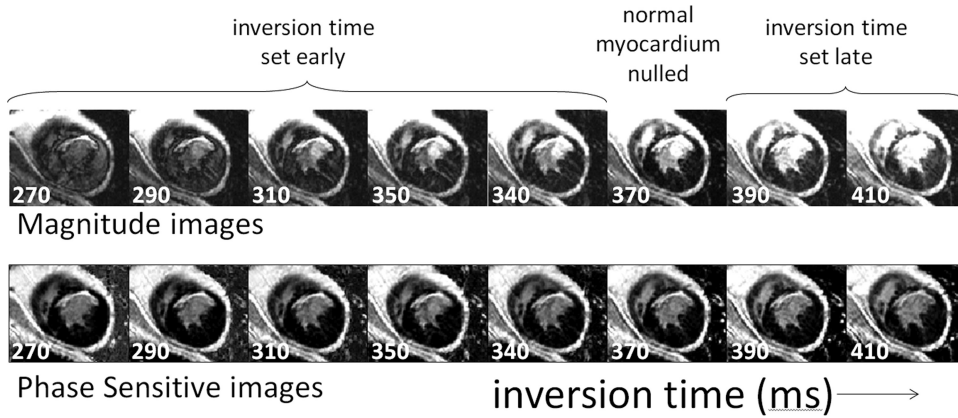Phase Sensitive images

inversion time (ms) ⟶

Figure 5. Magnitude IR (top) and PSIR (bottom) reconstructed late enhancement images acquired at a series of TIs illustrating the relative TI insensitivity of PSIR over a wide range.

acquisitions on a trial and error basis or by means of a cine-IR-SSFP scout (37) which acquired several TIs in a segmented manner, each at different cardiac phases. In this case, the null time may be underestimated because inversion recovery is influenced by the readout causing a shorter apparent T1 referred to as T1* (38), which depends on specific protocol parameters. Alternatively, a direct T1 mapping measurement may be made using a modified Look Locker inversion recovery (MOLLI) method (39) to determine appropriate TI to null the normal myocardium.

In cases for which the TI is set shorter than the time to null the normal myocardium, the loss of polarity in the magnitude reconstructed image will result in a loss of contrast. The positive signal may also appear as an artifact. PSIR reconstruction preserves polarity and is therefore much less sensitive to the inversion time (Fig. 5) (27,40,41). For PSIR late enhancement, the polarity is restored and may be retrospectively windowed and leveled to display the normal myocardium as black while the MI will appear bright.
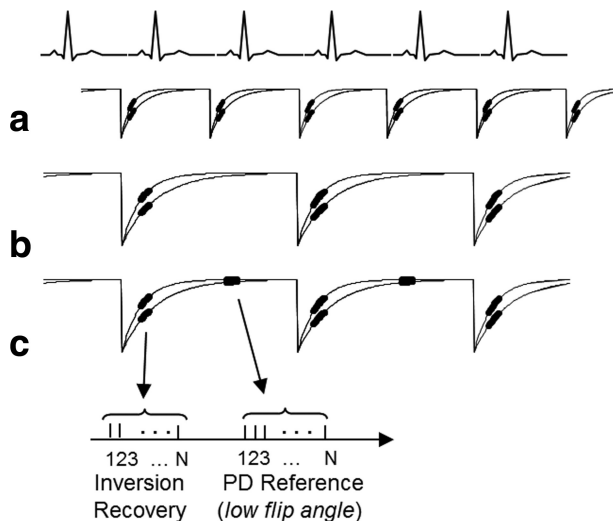
The 2D segmented IR-FLASH sequence (Fig. 6) is ECG triggered and may use inversions every R-R (Fig. 6a), or every 2 R-R intervals (Fig. 6b) to allow for more complete magnetization recovery (26,29). Using inversions every R-R with incomplete magnetization recovery will result in a reduction in signal intensity as well as greater sensitivity to variation in the R-R interval over the period of the breath-hold acquisition. Beat-to-beat variations in signal intensity that might arise to R-R variation may result in image artifacts (Fig. 7). For these reasons, triggering every 2 R-R intervals, or potentially 3 R-R intervals at high heart rates, is recommended. Of course, 2 R-R triggering requires a doubling of the acquisition time compared with single R-R triggering, and for this reason makes it impractical for most breathheld 3D protocols.

PSIR sequences typically acquire both an IR and a proton density (PD) weighted image at the same cardiac and respiratory phase to provide a reference for background phase, and for correcting surface coil intensity variation (27). With inversions every 2 R-Rs the PD image may be acquired on alternate heartbeats (Fig 6c) after the magnetization has substantially recovered and is essentially positive. A lower excitation flip angle for readout of the PD image is used to not steal too much of the magnetization and to better approximate a PD weighting.

Typical protocol parameters are listed in Table 1 for both segmented PSIR-FLASH and single shot PSIR-SSFP sequences. The magnitude IR and PSIR are essentially the same protocol, with the PSIR requiring the additional PD readout on alternate heartbeats. In the case of segmented PSIR-FLASH, the breath-hold

Figure 6. Timing of inversion recovery for (**a**) segmented IR with inversions every single R-R interval, (**b**) with inversions triggered every 2 R-R intervals, and (**c**) for segmented PSIR with inversions every 2 R-R intervals including acquisition of PD-weighted reference data on alternate heartbeats.
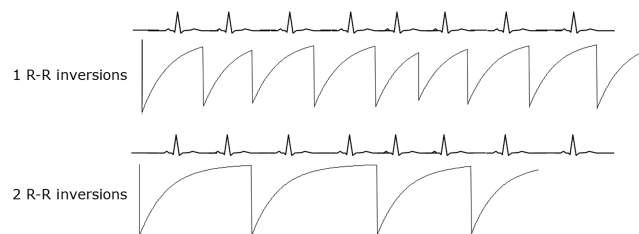

Figure 7. Using inversions every R-R interval leads to incomplete magnetization recovery. Sensitivity to R-R variations in single R-R triggering may lead to image artifacts as well as reduction of signal intensity.

Table 1
Typical Imaging Parameters for Segmented, PSIR-FLASH and Single Shot, PSIR-SSFP Late Enhancement Imaging Protocols

Protocol	Segmented, PSIR-FLASH	Single shot, PSIR-SSFP
Gadolinium dose	0.1-0.2 mmol/kg	
Time from dose	10-20 minutes	
Gating	ECG gated (diastolic)	
k-space acquisition	Linear interleaved order, segmented	Linear, single shot
Spatial resolution (typical)	1.4 x 1.9 x 6 mm^3 (256×144 matrix)	1.4 x 2.1 x 6 mm^3 (256×128 matrix)
TE/TR	3.9/8.5 ms	1.3/2.8 ms
Inversion time (TI)	250-300 ms	
Bandwidth	140 Hz/pixel	1000 Hz/pixel
Imaging window	145-200 ms (17-23 lines per segment)	180 ms using parallel imaging factor 2 (64 lines per shot)
IR preparation (non-selective)	Triggered every 2 R-R intervals	
Breathhold duration	14-18 heartbeats/slice (including 2 HB discarded) (8-10 heart beats using 2x accelerated parallel imaging)	2 heartbeats/slice
RF excitation flip angle	25° IR image (5° reference)	50° IR image (8° reference)

duration is directly related to the TR for a given segment duration. Asymmetric readout is commonly used in these protocols to minimize TE and TR. Maintaining a shorter TE maintains a more homogeneous blood pool, minimizing de-phasing to blood motion, however, as TE approaches the fat and water out-of-phase condition (2.3 ms at 1.5T) water/fat cancellation at borders may be problematic as discussed later. To decrease the breath-hold duration of segmented PSIR-FLASH acquisition for a given matrix size, it is possible to either increase the bandwidth, thereby reducing TE and TR, or to use parallel imaging. Both of these approaches entail a loss in SNR. For doubling the bandwidth the SNR loss is $\sqrt{2}$, and similarly is approximately $\sqrt{2}$ for parallel imaging with acceleration factor 2 assuming a surface coil array with adequate number of elements is used. This SNR loss may be acceptable for many applications but may not provide adequate image quality for demanding applications previously discussed, i.e., thin walls, subtle late enhancement patterns, or quantifying border zones.

Single Heart Beat Imaging and Motion Corrected Averaging

Single-shot, PSIR-SSFP may be used for rapid acquisition to acquire multiple 2D slices covering the entire heart in a single breath-hold (29), or may be used in cases of arrhythmias or difficulty breathholding when segmented breathhold scans may result in ghost artifacts (Fig. 8) (30–35). The SNR for single shot PSIR-SSFP is slightly worse than segmented PSIR-FLASH due to the increase in bandwidth, despite the increase in flip angle. However, the SNR of single shot PSIR-SSFP may be significantly improved by averaging multiple repeated measurements (Fig. 9). Motion corrected averaging may be used to correct respiratory motion (30,31) in the case of free-breathing acquisition, or diaphragmatic drift in the case of breathholding. Typically, using 8 frames acquired in 16 heartbeats provides an SNR comparable or better than the FLASH protocol for approximately the same duration and may be extended to a larger number of averages

because the acquisition is not breathheld. Parallel imaging at higher acceleration factors may be used to reduce the imaging duration in diastole to achieve higher spatial resolution or reduce motion blur at higher heart rates (Fig. 10). Use of nonrigid motion correction provides correction over the full FOV in a fully automated manner. Selective averaging may be used to discard images that do not meet similarity criteria due to through plane motion (31).

3D Late Enhancement Imaging

The widely used late enhancement protocol is 2D multislice requiring several breath-holds to obtain full heart coverage. Single breathhold 3D late enhancement with moderate resolution is possible and typically uses single R-R triggering and lengthier breath-holds (20–24 s) (42–44). Breath-held protocols use similar slice thickness (6–8 mm) to their 2D counterparts. Navigated free-breathing 3D protocols may achieve significantly higher spatial and temporal resolution as limited by SNR and acquisition time (5,45–

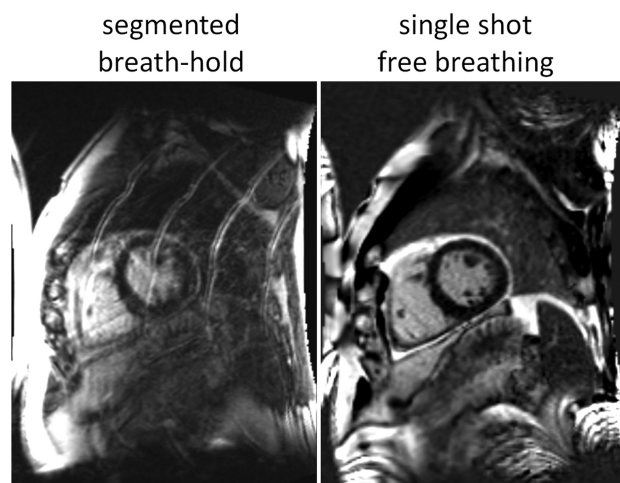segmented breath-hold   single shot free breathing

Figure 8. Illustration of respiratory ghost artifacts (left) segmented breathheld late enhancement imaging in situation where patient has difficulty holding their breath, which is mitigated using a single-shot free breathing protocol (right).
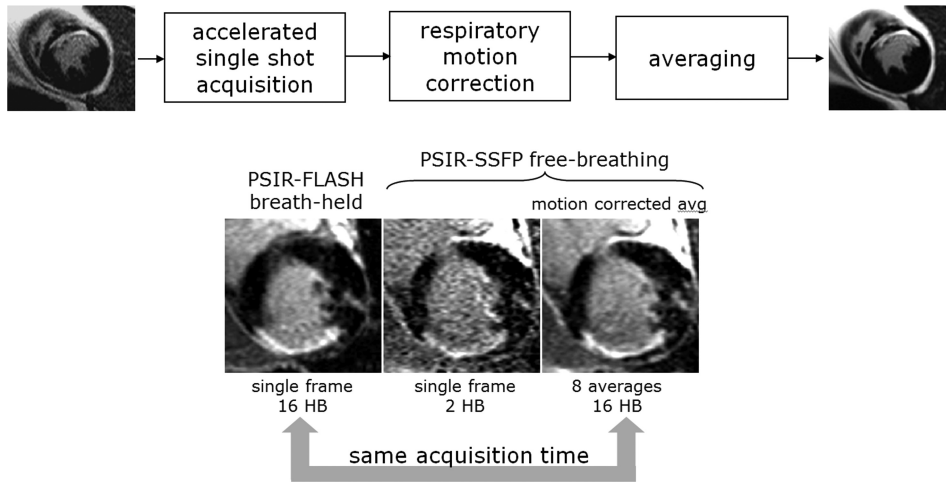
Figure 9. Respiratory motion corrected averaging of multiple accelerated single shot PSIR-SSFP images acquired during free-breathing may be used to improve the SNR becoming comparable or better than breath-held PSIR FLASH protocols for the same duration acquisition.

49). Navigated protocols may achieve slice thickness of 1.5–2 mm necessary to visualize small thin walled structures such as the atria (5,45) or to better visualize the detailed morphology of the MI such as the peri-infarct zone (50). Acquisition with isotropic resolution facilitates the prescription of nonangulated slabs, and retrospective display of normal cardiac views by means of multiplanar reformatting. The SNR for very thin slices (1.5 mm) is reduced and may require higher field strength (3T) for acceptable quality (46).

For segmented 3D acquisitions with high spatial resolution navigated scans are typically 5–10 min depending on the specific protocol and navigator efficiency. Consider the following example. With a TR of 5 ms and diastolic imaging duration of 150 ms, 50 phase encodes may be acquired each heartbeat. Thus for a matrix of $192 \times 256 \times 100$ (phase $\times$ read $\times$ slice), there would be 4 heartbeats per partition (slice) encode, which may be reduced to 2 heartbeats for parallel imaging factor 2. With 100 (noninterpolated) slices covering the heart 200 heartbeats must be acquired. Assuming a navigator efficiency of 35%, the acquisition duration would be approximately 10 min at nominal 60 bpm heart rate. This may be sped up by using partial Fourier acquisitions to reduce the number of phase encode and/or partition encodes or by using higher acceleration in parallel imaging, however, this is partially offset by the need for slice oversampling to avoid wrap due to imperfect slab excitation profile. The above calculation assumes inversions every R-R interval which comes at the cost of increasing the sensitivity to R-R variation and associated artifacts. Furthermore, most 3D protocols are not phase sensitive because PSIR methods typically require 2 R-R intervals between inversions would require doubling the acquisition time (49). As a result of Gd washout during the acquisition, it may be problematic to obtain an adequate null which may result in a loss of contrast and degradation of image quality.

Myocardium-to-Blood Pool Contrast

Late-enhancement imaging typically achieves excellent contrast between infarcted and normal myocar-

dium; however, the contrast between the MI and the blood pool is frequently suboptimal. Because a large fraction of infarctions caused by coronary artery disease are subendocardial, it is often difficult to assess the precise size of the infarct or to detect small infarcts. The contrast between the blood and MI in the inversion recovery image depends on variables such as contrast agent dosage, time from gadolinium administration, clearance rate, and imaging parameters. Blood velocity may also have a role in the contrast, even though non–slice-selective IR is used. Therefore, as a result of mechanisms that are not fully characterized or controlled, it is not infrequent that subendocardial MI are difficult to detect or clearly delineate.

Although imaging at a later time points may result in better blood pool contrast for some subjects (Fig. 11), it is generally not practical from the stand point of clinical workflow to wait too long, and in some instances may even result in poorer contrast. Technical solutions to this problem are to use multiple contrasts such as T1 and T2 (51,52), or to use blood suppression techniques (53). The T2 of blood (250 ms) is significantly longer than that of acute or chronic MI (50–70 ms) and may be used to discriminate the MI from blood pool. In the "Multicontrast delayed enhancement" (MCODE) approach (51), both T1- and
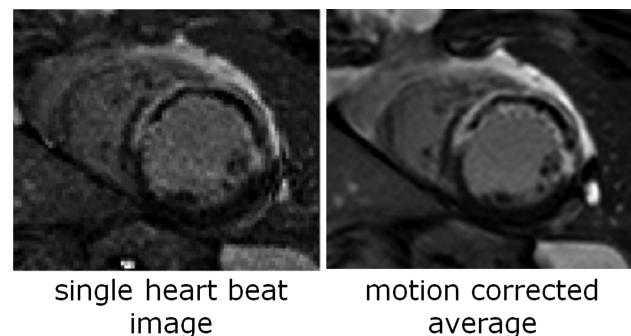

Figure 10. Example of PSIR late enhancement using motion corrected averaging with 256×144 matrix and 32 measurements. The diastolic imaging duration is less than 140 ms with parallel imaging acceleration factor 3.
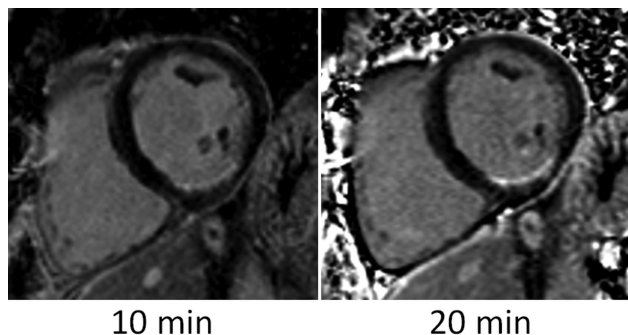
Figure 11. Contrast between MI and blood pool varies with time from gadolinium administration.

T2-weighted images are acquired within the same breath-hold. The T1-weighted image is a PSIR using either FLASH or SSFP readout, and the T2-weighted image uses an RF preparation for T2-weighting with effective TE = 40 ms. Both images are acquired at the same diastolic cardiac phase and are spatially registered facilitating fusion of the images to enhance the subendocardial border (Fig. 12). An alternative approach that also exploits the difference in tissue T1 and T2 is to use a segmented cine IR with SSFP readout (52). In this method, each cardiac phase has a unique T1 and T2 contrast as determined by both the inversion recovery and the SSFP readout which has a $\sqrt{T1/T2}$ steady state dependence. The blood will appear dark at a different cardiac phase than the MI. In an alternative approach, the IR-FLASH sequence may be modified to null both the blood and the normal myocardium using 2 inversions with carefully chosen inversion times (53). This scheme has been shown to provide contrast between the MI and the blood pool at the expense of SNR.

Fat in Late Enhancement Imaging and Fat-Water Separated Imaging

The presence of fibrofatty infiltration or other intramyocardial fat may have diagnostic value. Histological evidence of fibrofatty infiltration is a hallmark of arrhythmogenic right ventricular dysplasia (ARVD), and is also evident in chronic myocardial infarction (MI) and other nonischemic cardiomyopathies. The presence of intramyocardial fat may form a substrate for arrhythmias (54,55) due to the lower electrical conductivity of fat. It has been shown that fibrofatty infiltration of the myocardium is associated with sudden death (56), and, therefore, noninvasive detection could have high prognostic value.

Using conventional late enhancement imaging, it is difficult to discriminate between fibrosis and intramyocardial fat because both have low T1 and appear bright. Furthermore, the presence of fat may create image artifacts due to the chemical shift of fat or the bright epicardial fat signal may obscure the subepicardium. Using fat-water separated late-enhancement imaging it is possible to distinguish the fibrosis from fat (57–59) with improved sensitivity and to avoid erroneous tissue classification.

Fat-water-separated imaging may be combined with PSIR-FLASH using an inversion recovery sequence with multiecho readout (57–59). The water and fat images are spatially registered because they are reconstructed from the same multiecho dataset thus providing positive correlation between fibrosis and fat. An example of fatty infiltration in chronic MI is shown in Figure 13. In this example, the presence of fatty infiltration is not apparent in the conventional late enhancement image due to the low percentage of fat in a voxel. In a second example of chronic MI (Fig. 14) with higher fraction of fat, the conventional late enhancement image has a dark core in the MI which
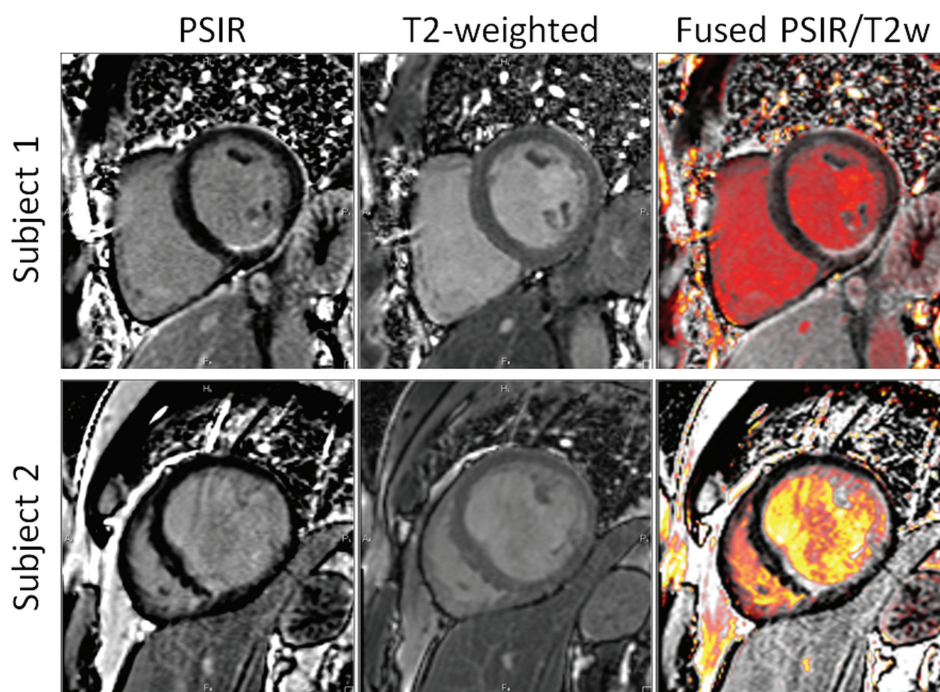

Figure 12. Multicontrast late enhancement (MCODE) acquired PSIR and T2-weighted images in the same breathheld acquisition at the same cardiorespiratory phase to enable discrimination between the blood and MI based on T2. Subject 1 (top) has excellent blood-to-MI contrast, while subject 2 has poor MI-to-blood contrast.
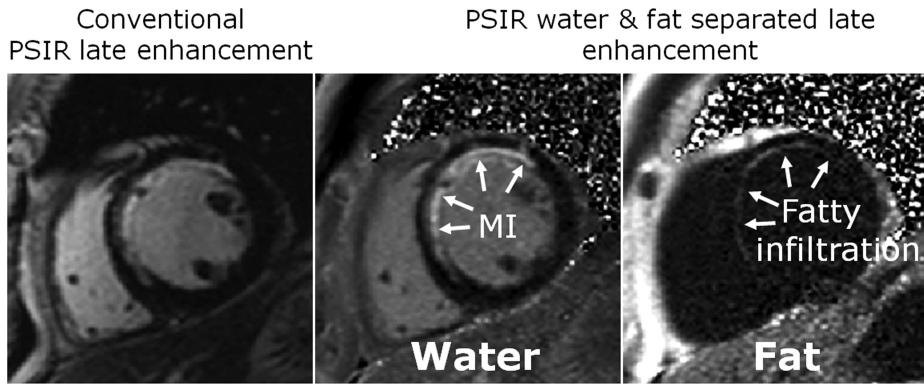
Conventional
PSIR late enhancement

PSIR water & fat separated late
enhancement

Figure 13. Example of fat water separated PSIR late enhancement illustrating fatty infiltration into chronic MI. Fatty infiltration is not evident in the conventional late enhancement for this subject.

appears erroneously as MVO frequently associated with acute MI. This region of water and fat appears dark on the conventional image due to cancellation between fat and water which are out of phase. In another example (Fig. 15), a lipomatous mass has the appearance of a chronic MI in conventional late enhancement, but is correctly determined to be fat using fat water separated late enhancement. Even in instances without intramyocardial fat, the epicardial fat will experience a chemical shift which can influence the interpretation. Conventional late enhancement imaging using 140 Hz/pixel has significant chemical shift artifact in which the fat is displaced relative to the water in the readout direction by approximately 1.5 pixels (at 1.5T). In this case, the epicardial fat may be displaced by as much as 30% of the diastolic wall thickness. In contrast, the multiecho fat-water-separated imaging approach, which uses a much larger bandwidth, has a subpixel shift (typically 0.2 pixel) and may be completely eliminated in the reconstruction by applying the known subpixel shift to the fat image.

The sequence used for fat-water separated imaging uses a multiecho readout and is reconstructed using a nonlinear estimation method which jointly solves for the water, fat, and fieldmap (60–62). A fat water separated late enhancement protocols using PSIR-FLASH at 1.5T would acquire each phase encode with a single echo train using monopolar readout with gradient flyback, number of echoes typically 4, bandwidth approximately 1,000 Hz/pixel, and echo spacing on order of 2.2 to 2.5 ms with TR approximately 10 to 11

ms. The overall breathhold duration for a segmented acquisition is approximately 30% longer than the conventional protocol for a fixed segment duration, thus it may be necessary to use parallel imaging to reduce the breathhold. Single shot, fat water separated PSIR-FLASH are possible using a readout with either two or three echoes and parallel imaging at an acceleration factors of 3 with motion corrected averaging to improve the SNR (63).

T1-Mapping and Extracellular Volume Fraction Mapping

Diffuse myocardial fibrosis is more difficult to distinguish using late gadolinium enhancement because the myocardial signal intensity is nearly constant and may be "nulled" thus appearing to be normal tissue. Quantitative measurement of the myocardial tissue longitudinal relaxation time constant (T1) following administration of extracellular Gadolinium contrast agent is sensitive to the increased extracellular volume associated with a globally diffuse myocardial fibrosis but has limitations due to a variety of confounding factors (64,65). Direct measurement of extracellular volume fraction (ECV) has been proposed as a means for detection and quantification of diffuse myocardial fibrosis (18,66,67). ECV mapping based on T1-maps acquired pre- and postcontrast calibrated by blood hematocrit circumvents the factors that confound T1-weighted images or T1-maps, and has been shown to correlate well with diffuse myocardial fibrosis.

conventional late enhancement   water   fat

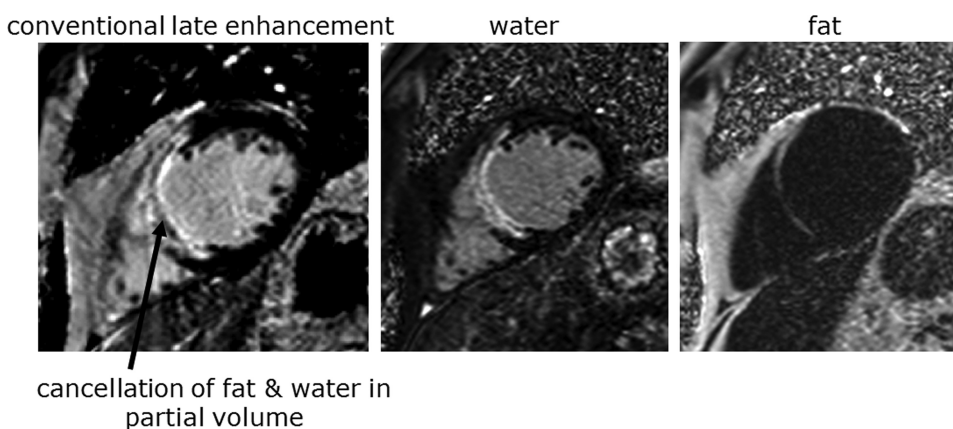cancellation of fat & water in
partial volume

Figure 14. Example of fatty infiltration of chronic MI which appears as a dark core MVO due to partial volume cancellation. Water and fat separated PSIR late enhancement images correctly classify the tissue into water and fat components.
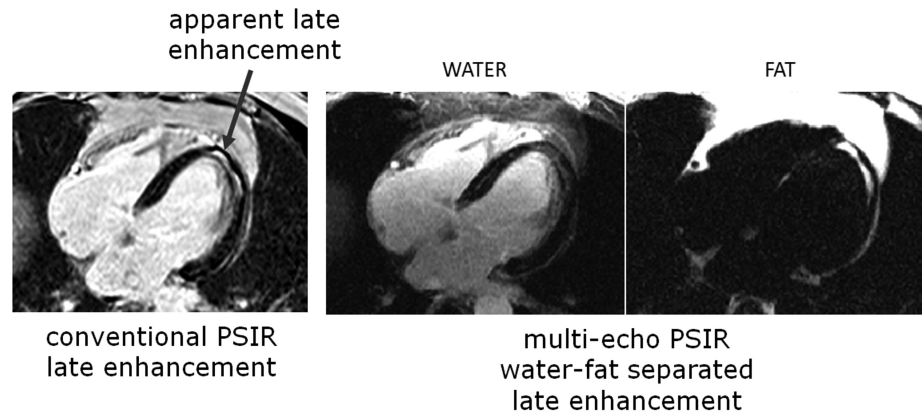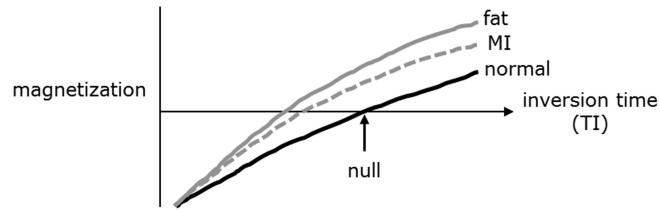
apparent late
enhancement

WATER   FAT

conventional PSIR
late enhancement

multi-echo PSIR
water-fat separated
late enhancement

Figure 15. A lipomatous mass has the appearance of a chronic MI in conventional late enhancement, but is correctly determined to be fat using fat water separated late enhancement.

Inversion recovery sequences for T1-mapping are similar to late enhancement imaging sequences. T1-mapping is based on inverting the magnetization and acquiring images at different times during the magnetization recovery, and performing a fit for model parameters at each pixel. For cardiac imaging, the acquisition is ECG triggered and all images are acquired at the same cardiac phase in late diastole using a Modified Look Locker Inversion Recovery (MOLLI) approach (39). This method has been extensively validated in human subjects across a wide range of heart rates and imaging protocols. Methods for T1-measurement such as cine inversion recovery (IR) (37,66) which acquire the measurements of magnetization at multiple cardiac phases may be used for measuring the T1 in the heart but are not suitable for mapping with pixel resolution. Following respiratory motion correction (described below), T1-fitting of the data at each pixel is performed by a nonlinear least square fit to the exponential recovery curve $abs(A–B\cdot exp(-TI/T1^*))$, where TI is the measured inversion time for each acquired image, the absolute value (abs) is used because the images are magnitude detected. $T1^*$ is the effective time constant which includes the effect of the image readout (38,39) related to the desired T1 as $T1=T1^* (B/A – 1)$. Motion correction may be used in T1-mapping using a synthetic reference scheme to deal with the changing image contrast (68).

Early Enhancement Imaging

The kinetics of gadolinium wash in may be imaged using a 2D multislice, single shot PSIR-SSFP single heart beat late enhancement protocol. With this protocol, it is possible to image the entire heart in a breath-hold, and is therefore clinically practical to acquire volumetric coverage during the early enhancement phase between 1 and 5 min following gadolinium administration, without tiring the patient. This time period is more sensitive to microvascular obstruction which may be less apparent at 10–20 min following Gd (Fig. 16).

Edematous myocardial tissue that may result from acute myocarditis or bordering acute MI (salvage area) will also have increased ECV and correspondingly higher concentration of gadolinium. In the case of acute MI, the edematous tissue will experience a more rapid early enhancement than the central core. Thus, in the case of acute MI, the early enhancement may show the area at risk (20).

Imaging Artifacts

As application of late enhancement imaging has widened, the demands on image quality have grown. Various approaches to late enhancement imaging have been described in the preceding sections which

1 min   2 min   3 min   4 min   5 min   6 min   7 min
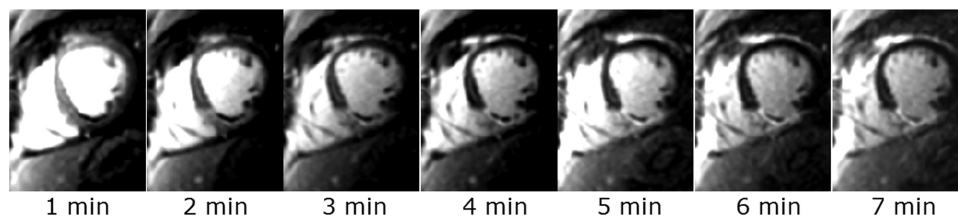
Figure 16. Time course of single shot PSIR SSFP for patient with acute MI during early enhancement when gadolinium washes in and fills the dark core region of microvascular obstruction.

address various issues including artifacts. Imperfect nulling of the normal myocardium in magnitude IR methods leads to both a loss of contrast as well as artifacts which may appears as patchy or mid-wall false enhancement. This issue is mitigated using the PSIR approach which restores the true signal polarity and can be retrospectively window-leveled to null the normal myocardium. Artifacts in inversion recovery imaging due to R-R variation may arise when using inversion every R-R interval which are reduced when increasing the interval between inversions. For significant arrhythmias, single shot imaging is recommended which avoids ghosting. Single shot imaging is also recommended in cases where patients have difficulty breathholding.

Artifacts due to fat are less well appreciated. These include cancellation between water and fat which may obscure fibrosis or lead to confusion, as well as a spatial displacement of fat due to chemical shift. Fat water separated late enhancement provides a means of mitigating artifacts due to fat as well as distinguishing intramyocardial fat which may be of diagnostic value.

Fluid regions such as pericardial effusion, cysts, or cerebral spinal fluid (CSF) with long T1 relaxation time may lead to ghosting in segmented protocols, and will appear bright on magnitude reconstructed images which might be confused with fat. The PSIR method is shown to correct the polarity of pericardial effusion (69,70), and the use of cardiac surface coil arrays with adaptive coil combining has been shown to reduce CSF ghosting (71) which in some instances might be confused with focal enhancement. Single shot methods avoid the problem of ghosting.

Loss of resolution or blurring may result due to a distorted "point spread function" due to a variety of factors. At higher heart rates cardiac motion blur will result in cases where the temporal resolution (segment duration) is too long. In this case, the segment duration must be reduced by reducing the number of lines per segment acquired or by reducing the TR by increasing the bandwidth. Increased bandwidth may result in a poor choice of echo time (TE) from fat cancellation standpoint, and will reduce the SNR as previously described. Point spread distortion may lead to edge enhancement when the segment is too long due to inversion recovery during the segment, but this is mitigated using PSIR reconstruction which discards the distorted imaginary component (27). Loss of effective in-plane resolution may result from using too large a slice thickness due to partial volume effects in the voxel (72). This may be minimized by using thinner 2D slices or by using 3D acquisitions.

Edge ringing may result from the so-called Gibb's effect which is due to truncating the measured k-space and may result in artifacts which mimic weaker mid-wall enhancement that might be confused with myocarditis. The use of "raw filters" or "windows" (e.g., Hamming or Hanning) which reduce the effect of hard truncation by softening or apodizing the measured data at edges of k-space will suppress this ringing at the expense of a slight loss in spatial resolution.

Measurement of Infarct Size

Quantitative measurement of infarct size is an important aspect of viability assessment. Computer assisted methods have been proposed to achieve an objective assessment that is less dependent on user selected window and level display parameters. Following segmentation of the myocardium, i.e., tracing the endo- and epicardial borders, approaches to measurement of the late enhanced infarcted region are usually based on either (a) setting a threshold above the noise as defined by a measurement in a remote region, or (b) setting a threshold at a value corresponding to full-width half maximum. Measurements of MI size based on the full-width half maximum approach have been shown to have high accuracy as validated with histology (6,8) whereas simple thresholding is subject to bias due to partial volume effects particularly due to slice thickness, and by high variability resulting from the generally small number of remote pixels as well as signal inhomogeneities that are attributed to noise. Furthermore, it is desirable to correct for surface coil intensity variation, particularly when using arrays of smaller elements, and in cases with larger infarcts. However, surface coil intensity correction (also referred to as normalization) converts a uniform noise image into a uniform sensitivity image which may introduce further bias errors for fixed thresholding methods that rely on uniform noise.

DISCUSSION

A variety of methods have been presented for late gadolinium enhancement imaging, spanning sequence design, image reconstruction technique, and acquisition strategy/protocols. These include (a) IR prepared sequences with FLASH or SSFP readout, (b) segmented or single shot readout, (c) magnitude versus phase sensitive reconstruction, (d) breathheld, navigated, or motion corrected averaging approaches, (e) single echo or multiecho Dixon like fat water separated imaging, (f) 2D multislice or 3D, and (g) T1-weighted versus T1-mapping. Each of the methods, have pros and cons, and some of these methods may not yet be generally available on all platforms. The breathheld, segmented IR prepared 2D multislice acquisition with FLASH readout, with either magnitude (26) or phase sensitive (27) reconstruction is widely available, is used by many institutions, and achieves high quality in a large proportion of cases. In cases where patients are unable to reliably breathhold or have significant arrhythmias, single shot approaches may be used with a free breathing acquisition. In conjunction with parallel imaging and respiratory motion corrected averaging, single shot free-breathing approaches provide a reliable solution with performance that is comparable in image quality, and spatial and temporal resolution to the breathheld segmented FLASH. As the demands for late gadolinium imaging has grown to encompass more challenging cases such as nonischemic cardiomyopathies or thin walled anatomical structures, the demands for reduced artifacts and higher spatial and temporal resolution has grown

correspondingly. The recent development of fat water separated late enhancement helps mitigate artifacts that arise due to fat, either intramyocardial fat or fat such as epicardial or pericardial fat in proximity to the myocardium of interest. Additionally, fat water separated imaging provides another a potentially important diagnostic tool for characterizing fibrofatty infiltration. 3D protocols are attractive for applications demanding high spatial resolution or to mitigate issues that arise due to partial volume effects.

CONCLUSION

Late gadolinium enhancement imaging is widely used and has become a standard for assessment of viability and general characterization of a broad range of both nonischemic and ischemic cardiomyopathies. As the number of applications has grown and encompass more subtle characteristics such as size and shape of the infarct border zone, or early detection of fibrosis, so have the demands for improved image quality. Methods for mitigating artifacts due to motion and/or arrhythmias have been developed which further increase the robustness of late enhancement imaging. The detection of fibrofatty infiltration or other intramyocardial fat is possible by means of fat-water separated late enhancement, which also serves to mitigate several artifacts that may arise due to the presence of fat.

High resolution 3D imaging is possible with longer navigated scans, however reliable imaging of small structures with the desired image quality remains challenging for clinical routine.

REFERENCES

1. Kim RJ, Fieno DS, Parrish TB, et al. Relationship of MRI delayed contrast enhancement to irreversible injury, infarct age, and contractile function. Circulation 1999;100:1992–2002.
2. Fieno DS, Kim RJ, Chen EL, Lomasney JW, Klocke FJ, Judd RM. Contrast-enhanced magnetic resonance imaging of myocardium at risk: distinction between reversible and irreversible injury throughout infarct healing. J Am Coll Cardiol 2000;36: 1985–1991.
3. Hunold P, Schlosser T, Vogt FM, et al. Myocardial late enhancement in contrast-enhanced cardiac MRI: distinction between infarction scar and non-infarction-related disease. AJR Am J Roentgenol 2005;184:1420–1426.
4. Bohl S, Wassmuth R, Abdel-Aty H, et al. Delayed enhancement cardiac magnetic resonance imaging reveals typical patterns of myocardial injury in patients with various forms of non-ischemic heart disease. Int J Cardiovasc Imaging 2008;24:597–607.
5. Vergara GR, Marrouche NF. Tailored management of atrial fibrillation using a LGE-MRI based model: from the clinic to the electrophysiology laboratory. J Cardiovasc Electrophysiol 2011;22:481–487.
6. Hsu L, Natanzon A, Kellman P, Hirsch GA, Aletras AH, Arai AE. Quantitative myocardial infarction on delayed enhancement MRI - Part I. Animal validation of an automated feature analysis and combined thresholding infarct sizing algorithm. J Magn Reson Imaging 2006;23:298–308.
7. Hsu L, Ingkanisorn WP, Kellman P, Aletras AH, Arai AE. Quantitative myocardial infarction on delayed enhancement MRI - Part II. Clinical application of an automated feature analysis and combined thresholding infarct sizing algorithm. J Magn Reson Imaging 2006;23:299–314.
8. Amado LC, Gerber BL, Gupta SN, et al. Accurate and objective infarct sizing by contrast-enhanced magnetic resonance imaging in a canine myocardial infarction model. J Am Coll Cardiol 2004; 44:2383–2389.
9. Yan AT, Shayne AJ, Brown KA, et al. Characterization of the peri-infarct zone by contrast-enhanced cardiac magnetic resonance imaging is a powerful predictor of post-myocardial infarction mortality. Circulation 2006;114:32–39.
10. Fernandes VR, Wu KC, Rosen BD, et al. Enhanced infarct border zone function and altered mechanical activation predict inducibility of monomorphic ventricular tachycardia in patients with ischemic cardiomyopathy. Radiology 2007;245:712–719.
11. Bluemke DA, Krupinski EA, Ovitt T, et al. MR imaging of arrhythmogenic right ventricular cardiomyopathy: morphologic findings and interobserver reliability. Cardiology 2003;99:153–162.
12. McCrohon JA, Moon JC, Prasad SK, et al. Differentiation of heart failure related to dilated cardiomyopathy and coronary artery disease using gadolinium-enhanced cardiovascular magnetic resonance. Circulation 2003;108:54–59.
13. Sen-Chowdhry S, Syrris P, Prasad SK, et al. Left-dominant arrhythmogenic cardiomyopathy: an under-recognized clinical entity. J Am Coll Cardiol 2008;52:2175–2187.
14. Moon JC, McKenna WJ, McCrohon JA, Elliott PM, Smith GC, Pennell DJ. Toward clinical risk assessment in hypertrophic cardiomyopathy with gadolinium cardiovascular magnetic resonance. J Am Coll Cardiol 2003;41:1561–1567.
15. Puchalski MD, Williams RV, Askovich B, et al. Late gadolinium enhancement: precursor to cardiomyopathy in Duchenne muscular dystrophy? Int J Cardiovasc Imaging 2009;25:57–63.
16. Kellman P, Hernando D, Shah S, et al. Myocardial fibro-fatty infiltration in Duchenne muscular dystrophy canine model detected using multi-echo Dixon method of water and fat separation imaging. Proc Intl Soc Mag Reson Med 2009;17:3762.
17. Maceira AM, Joshi J, Prasad SK, et al. Cardiovascular magnetic resonance in cardiac amyloidosis. Circulation 2005;111:186–193.
18. Arheden H, Saeed M, Higgins CB, et al. Measurement of the distribution volume of gadopentetate dimeglumine at echo-planar mr imaging to quantify myocardial infarction: comparison with 99mtc-dtpa autoradiography in rats. Radiology 1999;211:698–708.
19. Mahrholdt H, Wagner A, Judd RM, Sechtem U. Assessment of myocardial viability by cardiovascular magnetic resonance imaging. Eur Heart J 2002;23:602–619.
20. Matsumoto H, Matsuda T, Miyamoto K, Shimada T, Mikuri M, Hiraoka Y. Peri-infarct zone on early contrast-enhanced CMR imaging in patients with acute myocardial infarction. JACC Cardiovasc Imaging 2011;4:610–618.
21. Leung SW, Hsu L-Y, Berry C, Wilson J, Kellman P, Arai AE. Early gadolinium enhancement represents area at risk not infarct size: timing and kinetics are critical in interpreting MRI of acute myocardial infarction. In: Proceedings of the Annual Scientific Meeting of the American Heart Association, 2011. (abstract 16686).
22. Ugander M, Bagi PS, Oki AJ, et al. Myocardial edema as detected by pre-contrast T1 and T2 MRI delineates area at risk associated with acute myocardial infarction. JACC Cardiovasc Imaging. 2012 (in press).
23. Abdel-Aty H, Zagrosek A, Schulz-Menger J, et al. Delayed enhancement and T2-weighted cardiovascular magnetic resonance imaging differentiate acute from chronic myocardial infarction. Circulation 2004;109:2411–2416.
24. Wu KC, Zerhouni EA, Judd RM, et al. Prognostic significance of microvascular obstruction by magnetic resonance imaging in patients with acute myocardial infarction. Circulation 1998;97: 765–772.
25. Choi KM, Kim RJ, Gubernikoff G, Vargas JD, Parker M, Judd RM. Transmural extent of acute myocardial infarction predicts long-term improvement in contractile function. Circulation 2001; 104:1101–1107.
26. Kim RJ, Shah DJ, Judd RM. How we perform delayed enhancement imaging. J Cardiovasc Magn Reson 2003;5:505–514.
27. Kellman P, Arai AE, McVeigh ER, Aletras AH. Phase sensitive inversion recovery for detecting myocardial infarction using gadolinium delayed hyperenhancement. Magn Reson Med 2002;47: 372–383.
28. Simonetti OP, Kim RJ, Fieno DS, et al. An improved MR imaging technique for the visualization of myocardial infarction. Radiology 2001;218:215–223.
29. Huber A, Hayes C, Spannagl B, et al. Phase-sensitive inversion recovery single-shot balanced steady-state free precession for detection of myocardial infarction during a single breathhold. Acad Radiol 2007;14:1500–1508.

30. Kellman P, Larson AC, Hsu L, et al. Motion corrected free-breathing delayed enhancement imaging of myocardial infarction. Magn Reson Med 2005;53:194–200.

31. Ledesma-Carbayo MJ, Kellman P, Arai AE, McVeigh ER. Motion corrected free-breathing delayed enhancement imaging of myocardial infarction using nonrigid registration. J Magn Reson Imaging 2007;26:184–190.

32. Chung Y, Vargas J, Simonetti O, Kim R, Judd R. Infarct imaging in a single heart beat. J Cardiovasc Magn Reson 2002;4:12–13.

33. Huber A, Schoenberg SO, Spannagl B, et al. Single-shot inversion recovery TrueFISP for assessment of myocardial infarction. AJR Am J Roentgenol 2006;186:627–633.

34. Huber A, Bauner K, Wintersperger BJ, et al. Phase-sensitive inversion recovery (PSIR) single-shot TrueFISP for assessment of myocardial infarction at 3 tesla. Invest Radiol 2006;41:148–153.

35. Sievers B, Elliott MD, Hurwitz LM, et al. Rapid detection of myocardial infarction by subsecond, free-breathing delayed contrast-enhancement cardiovascular magnetic resonance. Circulation 2007;115:236–244.

36. Goldfarb JW, Shinnar M. Free-breathing delayed hyperenhanced imaging of the myocardium: a clinical application of real-time navigator echo imaging. J Magn Reson Imaging 2006;24:66–71.

37. Gupta A, Lee VS, Chung YC, Babb JS, Simonetti OP. Myocardial infarction: optimization of inversion times at delayed contrast-enhanced MR imaging. Radiology 2004;233:921–926.

38. Schmitt P, Griswold MA, Jakob PM, et al. Inversion recovery True-FISP: quantification of T(1), T(2), and spin density. Magn Reson Med 2004;51:661–667. Erratum in: Magn Reson Med 2004;52:698.

39. Messroghli DR, Greiser A, Frohlich M, Dietz R, Schulz-Menger J. Optimization and validation of a fully-integrated pulse sequence for modified look-locker inversion-recovery (molli) t1 mapping of the heart. J Magn Reson Imaging 2007;26:1081–1086.

40. Huber AM, Schoenberg SO, Hayes C, et al. Phase-sensitive inversion-recovery MR imaging in the detection of myocardial infarction. Radiology 2005;237:854–860.

41. Setser RM, Chung YC, Weaver JA, Stillman AE, Simonetti OP, White RD. Effect of inversion time on delayed-enhancement magnetic resonance imaging with and without phase-sensitive reconstruction. J Magn Reson Imaging 2005;21:650–655.

42. Foo TK, Stanley DW, Castillo E, et al. Myocardial viability: breath-hold 3D MR imaging of delayed hyperenhancement with variable sampling in time. Radiology 2004;230:845–851.

43. Kuhl HP, Papavasiliu TS, Beek AM, Hofman MB, Heusen NS, van Rossum AC. Myocardial viability: rapid assessment with delayed contrast-enhanced MR imaging with three-dimensional inversion recovery prepared pulse sequence. Radiology 2004;230:576–582.

44. Goetti R, Kozerke S, Donati OF, et al. Acute, subacute, and chronic myocardial infarction: quantitative comparison of 2D and 3D late gadolinium enhancement MR imaging. Radiology 2011; 259:704–711.

45. Peters DC, Wylie JV, Hauser TH, et al. Detection of pulmonary vein and left atrial scar after catheter ablation with three-dimensional navigator-gated delayed enhancement MR imaging: initial experience. Radiology 2007;243:690–695.

46. Amano Y, Matsumura Y, Kumita S. Free-breathing high-spatial-resolution delayed contrast-enhanced three-dimensional viability MR imaging of the myocardium at 3.0 T: a feasibility study. J Magn Reson Imaging 2008;28:1361–1367.

47. Saranathan M, Rochitte CE, Foo TK. Fast, three-dimensional freebreathing MR imaging of myocardial infarction: a feasibility study. Magn Reson Med 2004;51:1055–1060.

48. Nguyen TD, Spincemaille P, Weinsaft JW, et al. A fast navigator gated 3D sequence for delayed enhancement MRI of the myocardium: comparison with breathhold 2D imaging. J Magn Reson Imaging 2008;27:802–808.

49. Kino A, Zuehlsdorff S, Sheehan JJ, et al. Three-dimensional phase-sensitive inversion-recovery turbo FLASH sequence for the evaluation of left ventricular myocardial scar. AJR Am J Roentgenol 2009;193:W381–W388.

50. Peters DC, Appelbaum EA, Nezafat R, et al. Left ventricular infarct size, peri-infarct zone, and papillary scar measurements: a comparison of high-resolution 3D and conventional 2D late gadolinium enhancement cardiac MR. J Magn Reson Imaging 2009;30:794–800.

51. Kellman P, Chung Y, Simonetti OP, McVeigh ER, Arai AE. Multi-contrast delayed enhancement (MCODE) provides improved contrast between myocardial infarction and blood pool. J Magn Reson Imaging 2005;22:605–613.

52. Detsky JS, Stainsby JA, Vijayaraghavan R, Graham JJ, Dick AJ, Wright GA. Inversion-recovery-prepared SSFP for cardiac-phase-resolved delayed-enhancement MRI. Magn Reson Med 2007;58: 365–372.

53. Farrelly C, Rehwald W, Salerno M, et al. Improved detection of subendocardial hyperenhancement in myocardial infarction using dark blood-pool delayed enhancement MRI. AJR Am J Roentgenol 2011;196:339–348.

54. Molinari G, Sardanelli F, Zandrino F, et al. Adipose replacement and wall motion abnormalities in right ventricle arrhythmias: evaluation by MR imaging. Retrospective evaluation on 124 patients. Int J Card Imaging 2000;16:105–115. Erratum in Int J Card Imaging 2000;16:485.

55. Vignaux O, Lazarus A, Varin J, et al. Right ventricular MR abnormalities in myotonic dystrophy and relationship with intracardiac electrophysiologic test findings: initial results. Radiology 2002; 224:231–235.

56. Burke AP, Farb A, Tashko G, Virmani R. Arrhythmogenic right ventricular cardiomyopathy and fatty replacement of the right ventricular myocardium: are they different diseases? Circulation 1998;97:1571–1580.

57. Kellman P, Hernando D, Shah S, et al. Multi-echo Dixon fat and water separation method for detecting fibro-fatty infiltration in the myocardium. Magn Reson Med 2009;61:215–221.

58. Kellman P, Hernando D, Arai AE. Myocardial fat imaging. Curr Cardiovasc Imaging Rep 2010;3:83–91.

59. Goldfarb JW. Fat-water separated delayed hyperenhanced myocardial infarct imaging. Magn Reson Med 2008;60:503–509.

60. Reeder SB, Wen Z, Yu H, et al. Multicoil Dixon chemical species separation with an iterative least squares estimation method. Magn Reson Med 2004;51:35–45.

61. Reeder SB, Markl M, Yu H, Hellinger JC, Herfkens RJ, Pelc NJ. Cardiac CINE imaging with IDEAL water-fat separation and steady-state free precession. J Magn Reson Imaging 2005;22:44–52.

62. Hernando D, Kellman P, Haldar JP, Liang Z-P. Robust water/fat separation in the presence of large field inhomogeneities using a graph cut algorithm. Magn Reson Med 2010;63:79–90.

63. Kellman P, Hernando D, Shah S, Chefd'hotel C, Liang Z-P, Arai AE. Free-breathing, single shot fat-water separated cardiac imaging with motion corrected averaging. In: Proceedings of the 18th Annual Meeting of the ISMRM, Stockholm, 2010. (abstract 3662).

64. Mewton N, Liu CY, Croisille P, Bluemke D, Lima JA. Assessment of myocardial fibrosis with cardiovascular magnetic resonance. J Am Coll Cardiol 2011;57:891–903.

65. Gai N, Turkbey EB, Nazarian S, et al. T1 mapping of the gadolinium-enhanced myocardium: adjustment for factors affecting interpatient comparison. Magn Reson Med 2011;65:1407–1415.

66. Jerosch-Herold M, Sheridan DC, Kushner JD, et al. Cardiac magnetic resonance imaging of myocardial contrast uptake and blood flow in patients affected with idiopathic or familial dilated cardiomyopathy. Am J Physiol Heart Circ Physiol 2008;295: H1234–H1242.

67. Schelbert E, Testa SM, Meier CG, et al. Myocardial extracellular volume fraction measurement by gadolinium cardiovascular magnetic resonance in humans: slow infusion versus bolus. J Cardiovasc Magn Reson 2011;13:16.

68. Xue H, Shah S, Greiser A, et al. Motion correction for myocardial T1 mapping using image registration with synthetic image estimation. Magn Reson Med [Epub ahead of print].

69. Goldfarb JW, Arnold S, Schapiro W, Reichek N. On the cause of spatial displacement of long T1 species in segmented inversion recovery prepared imaging. Magn Reson Med 2005;54:481–485.

70. Dyke CK, Kellman P, Aletras AH, Arai AE. Pericardial effusion or epicardial fat? Improved discrimination with phase-sensitive inversion recovery MRI. J Cardiovasc Magn Reson 2003;5:279.

71. Kellman P, Dyke CK, Aletras AH, McVeigh ER, Arai AE. Artifact suppression in delayed hyperenhancement imaging of myocardial infarction using B1-weighted phased array combined phase sensitive inversion recovery. Magn Reson Med 2004;51:408–412.

72. Schelbert EB, Hsu LY, Anderson SA, et al. Late gadolinium-enhancement cardiac magnetic resonance identifies postinfarction myocardial fibrosis and the border zone at the near cellular level in ex vivo rat heart. Circ Cardiovasc Imaging 2010;3: 743–752.